Proton Availability at the Air/Water Interface

ARTICLE *in* JOURNAL OF PHYSICAL CHEMISTRY LETTERS · MAY 2010

Impact Factor: 7.46 · DOI: 10.1021/jz100322w · Source: OAI

3 AUTHORS, INCLUDING:

Michael R. Hoffmann
California Institute of Technology
379 PUBLICATIONS **30,162** CITATIONS

SEE PROFILE

Agustin J Colussi
California Institute of Technology
214 PUBLICATIONS **4,224** CITATIONS

SEE PROFILE

THE JOURNAL OF PHYSICAL CHEMISTRY Letters

pubs.acs.org/JPCL

Proton Availability at the Air/Water Interface

Shinichi Enami, Michael R. Hoffmann, and A. J. Colussi*

W. M. Keck Laboratories, California Institute of Technology, California 91125

ABSTRACT The acidity of the water surface sensed by a colliding gas is determined in experiments in which the protonation of gaseous trimethylamine (TMA) on aqueous microjets is monitored by online electrospray mass spectrometry as a function of the pH of the bulk liquid (pH_{BLK}). $TMAH^+$ signal intensities describe a titration curve whose equivalence point at pH_{BLK} 3.8 is dramatically smaller than the acidity constant of trimethylammonium in bulk solution, $pK_A(TMAH^+)$ = 9.8. Notably, the degree of TMA protonation above pH_{BLK} 4 is enhanced hundred-fold by submillimolar LiCl or NaCl and weakly inhibited at larger concentrations. Protonation enhancements are associated with the onset of significant direct kinetic solvent hydrogen isotope effects. Since TMA(g) can be protonated by H_2O itself only upon extensive solvent participation, we infer that H_3O^+ emerges at the surface of neat water below pH_{BLK} 4.

SECTION Atmospheric, Environmental and Green Chemistry

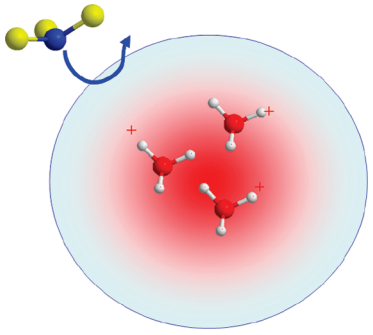

The peculiar features of gas/liquid processes and their critical roles in atmospheric chemistry remain incompletely understood.[1,2] Interfacial events proceed in the outermost layers of liquids as they thin into vapors, that is, in media that are nonuniform at the molecular scale and lack free-energy basins.[3,4] Some gases, such as ozone and hydroxyl radicals,[5] react with dissolved species in the interfacial layers, whereas others do so after becoming incorporated into the bulk liquid. These interfacial processes might be better approached from the gas- rather than condensed-phase properties of the participating species. The differential heats of chemisorption of gaseous alkylamines on acidic zeolite surfaces, for example, correlate with the gas-phase proton affinities rather than with amine pK_A's in solution.[6]

Since protons participate as reactants or catalysts in most gas/water processes, it would be useful to establish an acidity scale for the water surface. By analogy with pH in bulk water (pH_{BLK}) any such "pH_S" scale must be defined in terms of portable standard states and measurable properties associated with interfacial proton equilibria. The steep density gradient ($\sim 10^8$ g cm^{-4}) at the water surface[7,8] however requires probing proton exchange equilibria on the nanometer scale. Since the residence time of mass-accommodated species in the outermost layers is spontaneously limited to the nanosecond range by desorption or diffusion, only the fastest chemical reactions may properly respond to interfacial acidity. Less reactive gases, after settling on the surface, will diffuse into and sense the acidity of bulk water instead. We believe that the conflicting interpretations of the statement "water surface is acidic"[9] reflect these issues and call for an operational definition of "surface acidity".

Consider the hydrolysis of trimethylamine, TMA, "on water". Gas-phase proton affinities: PA(TMA) = 227 kcal mol^{-1} and $PA(H_2O)$ = 165 kcal mol^{-1}, and the acidity constant of its conjugated acid in aqueous solution: $pK_A(TMAH^+)$ = 9.8, suggest that TMA is a stronger base than H_2O in both the gas and liquid phases. However, reaction 1

$$H_3O^+(g) + TMA(g) \rightarrow TMAH^+(g) + H_2O(g) \quad (1)$$

$$H_2O(g) + TMA(g) \rightarrow TMAH^+(g) + OH^-(g) \quad (2)$$

is exothermic, ΔH_1 = PA(TMA) − $PA(H_2O)$ = −62 kcal mol^{-1}, whereas reaction 2 is not, ΔH_2 = 164 kcal mol^{-1}.[10,11] Reaction 2 actually becomes viable only after its ion products are extensively hydrated.[12,13] Thus, thermochemistry alone suggests that the degree of TMA protonation (>99% at pH_{BLK} 7) in bulk neutral water should sharply decrease at the air/water interface. "To what extent is TMA protonated upon alighting on the water surface" is therefore a valid question that can be addressed experimentally.[14] The dependence of the extent of TMA protonation on pH_{BLK} in gas/water collisions provides an operational measure of interfacial proton availability that avoids the ambiguities associated with pseudothermodynamic pH_S scales based on surface-specific spectroscopic signatures or model calculations. Below, we report novel experimental results on the protonation of TMA on water surfaces.

In our experiments, gas/liquid interactions take place on the surface of aqueous microjets injected (through an electrically grounded nozzle) into the spraying chamber of an electrospray ionization mass spectrometer (ESI-MS) flushed with TMA(g)/N_2(g) mixtures at 1 atm and 293 K (see Experimental Methods, Figure S1, in Supporting Information,

Received Date: March 12, 2010
Accepted Date: April 26, 2010

DOI: 10.1021/jz100322w | *J. Phys. Chem. Lett.* **2010**, *1*, 1599–1604

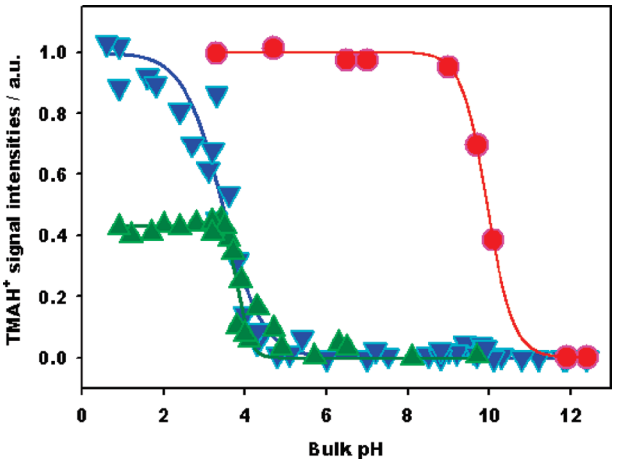

Figure 1. ESI-MS $TMAH^+$ signal intensities versus pH_{BLK} on water microjets exposed to 1.0−3.0 (blue downward triangles) and 0.03 ppmv TMA(g) (green upward triangles) and on aqueous $TMAH^+$-Cl^- microjets in pure N_2(g) (red circles). Blue and red signal intensity data are normalized to $TMAH^+$ = 1 at pH_{BLK} = 1. Green data are relative to the blue data. All experiments are at 1 atm and 293 K.

SI).[15,16] The fast nebulizer gas shreds the interfacial layers of the microjet into microdroplets. The kinetic energy dissipated in this process overcomes not only liquid cohesion but electrostatic attraction among anions and cations. Hence, microdroplets carry net charges even when generated from an electrically neutral liquid in the absence of an external electric field. Thus, in our experiments (1) ESI-MS $TMAH^+$ signal intensities report the $TMAH^+$ excesses carried by positively charged microdroplets, (2) $TMAH^+$ excesses are expected to be proportional to [$TMAH^+$] in the interfacial layers of the microjet, and (3) the $TMAH^+$ excesses carried by the analyzed microdroplets are conserved during water or TMA evaporation or in collisions with neutral TMA(g). We verified that this setup actually behaves as a linear transfer device, that is, ESI-MS signals are directly proportional to ion concentrations (in the submillimolar range, Figure S2, SI) in the interfacial layers of the microjet.[17−19] For example, the titration curves of aqueous *n*-hexanoic and *n*-octanoic acid obtained from anion concentrations, [A^-], determined in this setup were found to adhere to eq 3

$$\frac{[A^-]}{[A]_T} = \frac{1}{1 + 10^{pK_A - pH_{BLK}}} \qquad (3)$$

with the pK_A (*n*-hexanoic acid) = 4.81 ± 0.05 and pK_A (*n*-octanoic acid) = 4.81 ± 0.06 values reported in bulk solution.[20] This finding confirms that the degree of dissociation of these weak acids determined from A^- signal intensities measured by ESI-MS of negatively charged microdroplets reflects the pH_{BLK} of the microjet rather than the (presumably variable) acidity of evaporating microdroplets en route to the detector. In this manner, the $TMAH^+$ ions already present in the injected solutions or those produced in situ on the surfaces of microjets in contact with TMA(g) are detected and quantified by online ESI-MS within 1 ms.

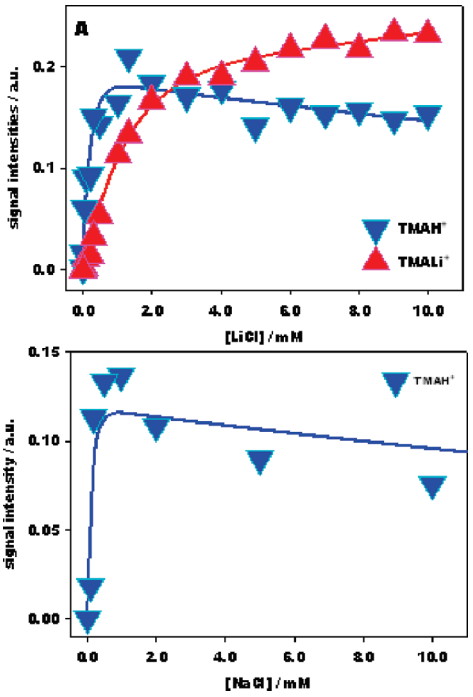

Figure 2. (A) ESI-MS $TMAH^+$ (*m*/*z* = 60, blue downward triangles) and $TMALi^+$ (*m*/*z* = 66, red upward triangles) signal intensities from aqueous LiCl microjets as functions of [LiCl] at pH_{BLK} 6.5. (B) $TMAH^+$ (*m*/*z* = 60, blue downward triangles) signal intensities from aqueous NaCl microjets at pH_{BLK} 7.8 as functions of [NaCl]. All experiments are under 1 ppmv TMA(g).

Positive ion electrospray ionization mass spectra of microjets produced by spraying water (previously adjusted to various pH_{BLK} values using HCl or NaOH) display $TMAH^+$ (*m*/*z* = 60) and $(TMAH)_2Cl^+$ (*m*/*z* = 155, 157) signals (Figure S3, SI) after being briefly exposed to TMA(3.0 ppmv)/N_2(1 atm) mixtures (see below for effective exposure times). At constant [TMA(g)], $TMAH^+$ signal intensities vary with pH_{BLK}, as shown in Figure 1 (blue downward triangles). A fit of eq 3 to experimental data yields $pK_A(1) = 3.8 \pm 0.2$. In Figure S4 (SI), it is possible to discern that $TMAH^+$ signals actually drop ∼100 times from $pH_{BLK} \approx 1$ to $pH_{BLK} \approx 5$, recover 10-fold at $pH_{BLK} \approx 9.5$, and fall off again above $pH_{BLK} \approx 10$. $TMAH^+$ signals (as well as *m*/*z* = 61 HCO_3^- signals from possible contamination by ambient CO_2) remain below the detection limit in experiments on deionized water. Previous reports for the uptake of NH_3(g) on aqueous train droplets reveal similar behavior about $pK_A(NH_4^+) = 9.25$.[21,22]

In striking contrast, $TMAH^+$ signals from $TMAH^+Cl^-$ solutions sprayed in pure N_2(g) vary with pH_{BLK} along a titration curve (red circles in Figure 1) whose equivalence point, $pK_A(2) = 9.96 \pm 0.02$, overlaps the reported $pK_A(TMAH^+) = 9.8 \pm 0.2$ value in bulk solution.[12,13] The data of Figure 1 represent direct evidence that protons are as available to TMA(g) at the surface of water at $pH_{BLK} \approx 3.8$ as they are to TMA(aq) in bulk solution at $pH_{BLK} \approx 9.8$. Thus, (1) TMA is more basic than water in the gas and bulk liquid phases but not at the interface and (2) the proton activity sensed by TMA(g) at the air/water interface is indirectly related to pH_{BLK}.

DOI: 10.1021/jz100322w | J. Phys. Chem. Lett. 2010, 1, 1599–1604

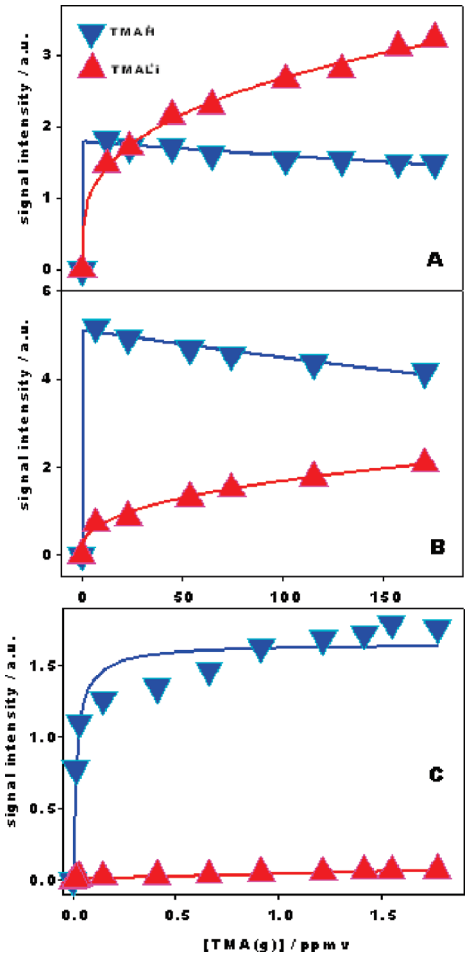

Figure 3. ESI-MS $TMAH^+$ (m/z = 60, blue downward triangles) and $TMALi^+$ (m/z = 66, red upward triangles) signal intensities on 100 mM aqueous LiCl microjets at (A) pH_{BLK} 3.5 and (B and C) pH_{BLK} 2.0, as functions of [TMA(g)].

We found that the negligible uptake of TMA(g) on near-neutral aqueous microjets is dramatically enhanced by sub-millimolar inert electrolytes such as LiCl and NaCl. (Figure 2). The promoting effects of LiCl and NaCl peak at ~1 mM and weakly decline at larger concentrations. In more acidic (pH_{BLK} < 5) water and at larger concentrations, Li^+ competitively binds TMA(g) as $TMALi^+$ (m/z = 66) instead (Figures S5 and S6, SI). The dissimilar dependences of $TMAH^+$ and $TMALi^+$ signal intensities on TMA(g) concentration in acidic water (Figure 3), together with the titration curves obtained under 0.03 and 1.0–3.0 ppmv TMA(g) of Figure 1, imply that TMA(g) is exclusively protonated by H_3O^+ rather than by H_2O in the outermost interfacial layers of the aqueous microjets. Since the limiting $TMAH^+$ signal intensities reached under 0.03 ppmv TMA(g) are only 43% of those obtained at ~100 times larger TMA(g) number densities (at pH_{BLK} < 3; Figure 1), uptake is limited by TMA(g) in the former case and by interfacial protons above 1.0 ppmv TMA(g). This finding is corroborated by the observation that $TMAH^+$ signals plateau above ~0.3 ppmv TMA(g) at pH_{BLK} 2.0, while $TMALi^+$ signals keep increasing at larger TMA(g) concentrations (Figure 3C).

Since the partial depletion of TMA near the air/water interface should have affected both $TMAH^+$ and $TMALi^+$ signals, the observed behaviors exclude significant resistance from gas-phase diffusion to TMA(g) uptake under present conditions. A limited role for gas-phase diffusion cannot be technically excluded, however, because all experiments were performed on aqueous microjets of similar dimensions under 1 atm of total pressure.

Perhaps not coincidentally, LiCl and NaCl enhance TMA protonation (Figure 2) in the same concentration range in which the surface tension of aqueous electrolytes dips to a minimum (the Jones–Ray effect).[8,23,24] Since the Debye screening length is > 3 nm at the onset of electrolyte effects at 0.1 mM (Figure 2),[25] both phenomena seem to manifest short-range forces associated with the local structure of interfacial water.[26−29] It could tentatively be argued that Li^+ and Na^+ replace protons as counterions in the diffuse electric double layer,[25] thereby releasing them to the surface.[30] Alternative explanations are being explored experimentally in our laboratory.

Our results constrain the duration of molecular TMA(g)/water encounters, the time microjet surfaces are effectively exposed to TMA(g), and the thickness of the interfacial layers probed in these experiments. By assuming that (1) the proton concentration reaches its bulk value at an interfacial depth of $\delta \approx 1.0$ nm below the Gibbs dividing surface (GDS) and (2) the pseudo-first-order diffusionally controlled rate constant, ${}^{I}k_P$, for the protonation of neutral TMA lying outside of the GDS is given by the Debye–Smoluchowski's equation, ${}^{I}k_P = 4\pi(D_{H^+} + D_{TMA})R_{TMA+H^+}[H^+]$[31] (where $D_{H^+} = 5 \times 10^{-4}$ cm^2 s^{-1} is the proton diffusion coefficient at the interface,[32] $D_{TMA} \approx 1.5 \times 10^{-5}$ cm^2 s^{-1} is the TMA diffusion coefficient, and $R_{TMA+H^+} = 5 \times 10^{-8}$ cm is the distance of closest approach), we estimate ${}^{I}k_P = 2 \times 10^7$ s^{-1} at pH_{BLK} 4.0. Minimal protonation of TMA(g) at pH_{BLK} 4.0 (see Figure 1) therefore implies that the first-order rate constant for TMA desorption, ${}^{I}k_D$, must be ~10 times larger than ${}^{I}k_P$. The derived duration of TMA(g)/water contacts, $\tau_D = 1/{}^{I}k_D < 1/(10\,{}^{I}k_P) \approx 5$ ns, is consistent with estimates based on transition state theory and the free energy of TMA adsorption on water[33] and with some MD simulations.[34] The effective time, τ_E, that the probed microjet surfaces are exposed to TMA(g) can be estimated from the surface density, S_{H^+}, of the protons titrated by 0.3 ppmv TMA(g) at pH_{BLK} 2.0 during τ_E (Figure 3C) and the TMA(g)/water surface collision rate, f, $\tau_E = S_{H^+}/f$. We assume that S_{H^+} is given by $S_{H^+} = [H^+]_{BLK} \times \delta = 6 \times 10^{18}$ protons cm^{-3} $\times$ 1 $\times$ 10^{-7} cm = 6×10^{11} protons cm^{-2}, and f is given by $f = (1/4)\gamma \times c \times n = 6.8 \times 10^{16}$ molecules cm^{-2} s^{-1} [where γ < 1 is the TMA(g) uptake coefficient, $c = 3.7 \times 10^4$ cm s^{-1} is the mean molecular speed of TMA(g) at 300 K, and $n = 7.3 \times 10^{12}$ TMA(g) molecules cm^{-3}].[35] Hence, $\tau_E < 6 \times 10^{11}$ protons cm^{-2}/6.8×10^{16} molecules cm^{-2} s^{-1} = 9 μs. Note that proton replenishment of the $\delta \approx 1.0$ nm interfacial layer by diffusion from the bulk during τ_E will be opposed by the electrostatic field created by the buildup of $TMAH^+$ positive charge at the interface. More precise kinetic estimates are beyond present instrumental design and procedures.

Figure 4 shows the results of experiments in which the ratio of $TMAH^+/TMAD^+$ signal intensities was determined (1) by

DOI: 10.1021/jz100322w | J. Phys. Chem. Lett. 2010, 1, 1599–1604

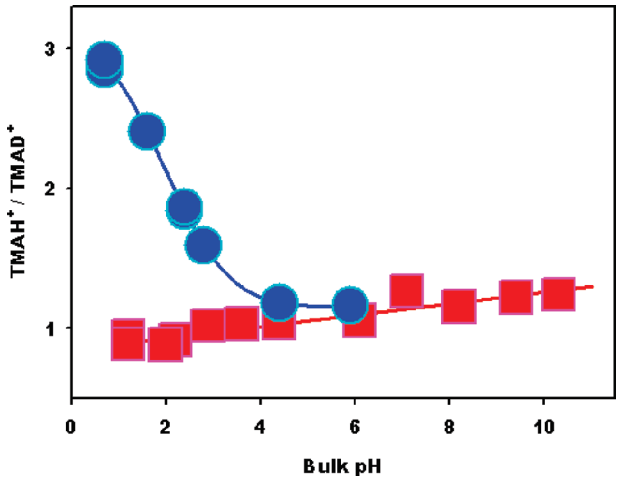

Figure 4. The $TMAH^+(m/z = 60)/TMAD^+(m/z = 61)$ ESI-MS signal ratio as a function of pH_{BLK}. Blue circles are from H_2O/D_2O (50:50) microjets exposed to 1 ppmv TMA(g). Red squares are from $TMAH^+Cl^-$ solutions in H_2O/D_2O (50:50).

exposing H_2O/D_2O (50:50) (vol:vol) microjets to TMA(g) or (2) by spraying 0.8 mM $TMAH^+Cl^-$ solutions in H_2O/D_2O (50:50) in pure N_2(g) as a function of pH_{BLK}. Significant direct kinetic hydrogen isotope effects were only observed in the first set of experiments at $pH_{BLK} \leq 4.5$ and also at $pH_{BLK} \approx 7$ in the presence of Li^+ or Na^+ ($TMAH^+/TMAD^+ = 1.0$ on H_2O/D_2O (50:50) at $pH_{BLK} = 6.7$; $TMAH^+/TMAD^+ = 3.2$ upon addition of 100 mM LiCl or NaCl at $pH_{BLK} = 6.5$).

We infer that (1) H/D are fully scrambled prior to analyzing $TMAH^+Cl^-$ solutions in H_2O/D_2O and (2) the enhanced TMA(g) protonation on water surfaces at $pH_{BLK} < 4$ and on Li^+/Na^+ solutions at $pH_{BLK} > 5$ is due to the faster protonation of adsorbed TMA molecules. Additional evidence that our experiments actually monitor interfacial chemical events follows from the $TMAH^+/TMAD^+ \approx 1/4$ ratio measured on neat D_2O microjets at pH_{BLK} 3, exposed to 1 ppmv TMA(g) humidified with ~250 ppmv H_2O(g). A much smaller $TMAH^+/TMAD^+ <$ 1/40 value should have been measured if incoming H_2O(g) had undergone full H-isotope scrambling with microjet bulk D_2O.

The widely separated titration curves of Figure 1 reveal that the conjugated species TMA(g) and $TMAH^+$ experience markedly different molecular environments on the opposite sides of the air/water interface. The energy for binding a water molecule to a $Y(H_2O)_n^{\pm}$ ion cluster converges, in general, to the enthalpy of vaporization of bulk water (ΔH_v = 10.5 kcal mol^{-1}),[10,11,36,37] while the hydration enthalpies of the $Y(H_2O)_n^{\pm}$ clusters reach ~(−70 ± 3) kcal mol^{-1} above $n > 4$.[11] Neutral TMA weakly (4.5 kcal mol^{-1}) binds only one water molecule.[38] Thus, the cumulative binding energies of the $TMAH(H_2O)_3^+$ (37.8 kcal mol^{-1})[36] and $OH(H_2O)_5^-$ (84.3 kcal mol^{-1})[10,39,40] clusters is still ~42 kcal mol^{-1} short of the stabilization required to overcome the endothermicity of reaction 2. Since product ions may not be stabilized further at the reduced interfacial water densities, TMA may not be protonated on water surfaces from which H_3O^+ were initially absent. Note that water autoionization is a slow, activated process (ΔG_d = 21.4 kcal mol^{-1}, $\Delta G^{\ddagger}$ = 23.8 kcal mol^{-1}) driven by infrequent (~10^{-4} s^{-1}) solvation energy fluctuations[41] that will not resupply protons during short TMA residence times ($\tau_D < 10$ ns, see above).

The results of Figure 1 suggest an isoelectric point $pK_{ISO} = pK_A(1) = 3.8 \pm 0.2$ for the water surface, in good agreement with the value derived from electrophoretic experiments on bubbles and droplets in water.[27,42,43] The preferential segregation of hydroxide at the water surface may be another example of anion enrichment at water/hydrophobic media interfaces.[18,26,44,45] The most recent phase-sensitive sum frequency vibrational spectroscopic (PS-SFVS) studies[4] also support the notion that OH^- adsorbs more strongly than H_3O^+ to water/hydrophobic media interfaces. The pH_{BLK} dependence of the imaginary component Im $\chi_S^{(2)}$ of the complex nonlinear susceptibility $\chi_S^{(2)}$ associated to the "ice-like" ~3200 cm^{-1} O−H band on the water/octadecyltrichlorosilane (OTS) interface leads to $pK_{ISO} \approx 3.0-3.2$ (water/vapor surfaces might behave similarly, but it remains to be confirmed).[46,47] This conclusion is reached by assuming that the sign of Im $\chi_S^{(2)}$ reflects the direction of the molecular dipole moment.[48] Positive Im $\chi_S^{(2)}$ values indicate outwardly pointing O−H groups on water surfaces negatively charged by preferential OH^- adsorption.[4] A more detailed analysis, however, shows that positive Im $\chi_S^{(2)}$ values result from collective orientational correlations rather than from the properties of discrete molecular moieties on the water surface.[48] The advent of phase-sensitive measurements implies that previous descriptions of the structure of the water surface drawn from SHG or SFVS$|\chi_S^{(2)}|^2$ data await critical reexamination.[28,49−52] The jury is still out on how spectroscopic signals relate to interfacial proton activity/reactivity on water surfaces.[26]

Multistate empirical valence bond calculations reveal that a single excess proton (plus a chloride counterion) in a slab of 500 water molecules (i.e., in $pH_{BLK} \approx 1$ water) has statistical preference for the interface.[53,54] First-principles molecular dynamics calculations for a hydroxide anion in 215 water molecules ($pH_{BLK} \approx 13$) suggest marginal stabilization at the air/water interface (by ~0.6 versus < 3 kcal mol^{-1} for the still-favored excess protons) relative to the bulk.[55] Some MD calculations based on polarizable force fields predict that OH^- is repelled from the water surface,[56,57] whereas others reach the opposite conclusion.[58] Since both H_3O^+ and OH^- are amphiphilic,[59] forthcoming model calculations should rationalize the larger affinity of OH^- for the water surface in the critical $4 < pH_{BLK} < 7$ range at issue.

Summing up, experiments show that trimethylamine molecules colliding with water surfaces are protonated only if the bulk liquid had been acidified to $pH_{BLK} < 4$. Protons are as available to TMA(g) at the surface of water at $pH_{BLK} \approx 3.8$ as they are to TMA(aq) in bulk solution at $pH_{BLK} \approx 9.8$.

SUPPORTING INFORMATION AVAILABLE

Additional data and experimental details. This material is available free of charge via the Internet at http://pubs.acs.org.

AUTHOR INFORMATION

Corresponding Author:

*To whom correspondence should be addressed. E-mail: ajcoluss@caltech.edu.

DOI: 10.1021/jz100322w | J. Phys. Chem. Lett. 2010, 1, 1599–1604

ACKNOWLEDGMENT S.E. appreciates the Japan Society for the Promotion of Sciences Postdoctoral Fellowships for Research Abroad. We thank Nathan Dalleska for expert help with some experiments. This work was supported by National Science Foundation Grant ATM-0714329.

REFERENCES

(1) Finlayson-Pitts, B. J. Reactions at Surfaces in the Atmosphere: Integration of Experiments and Theory as Necessary (but Not Necessarily Sufficient) for Predicting the Physical Chemistry of Aerosols. *Phys. Chem. Chem. Phys.* **2009,** *11*, 7760–7779.

(2) Garrett, B. C.; Schenter, G. K.; Morita, A. Molecular Simulations of the Transport of Molecules Across the Liquid/Vapor Interface of Water. *Chem. Rev.* **2006,** *106*, 1355–1374.

(3) Bian, H. T.; Feng, R. R.; Guo, Y.; Wang, H. F. Specific Na^+ and K^+ Cation Effects on the Interfacial Water Molecules at the Air/Aqueous Salt Solution Interfaces Probed with Nonresonant Second Harmonic Generation. *J. Chem. Phys.* **2009**, *130*, doi: 134709 10.1063/1.3104609.

(4) Tian, C. S.; Shen, Y. R. Structure and Charging of Hydrophobic Material/Water Interfaces Studied by Phase-Sensitive Sum-Frequency Vibrational Spectroscopy. *Proc. Natl. Acad. Sci. U.S. A.* **2009,** *106*, 15148–15153.

(5) Bagot, P. A. J.; Waring, C.; Costen, M. L.; McKendrick, K. G. Dynamics of Inelastic Scattering of OH Radicals from Reactive and Inert Liquid Surfaces. *J. Phys. Chem. C* **2008,** *112*, 10868–10877.

(6) Parrillo, D. J.; Gorte, R. J.; Farneth, W. E. A Calorimetric Study of Simple Bases in H-ZSM-5: A Comparison with Gas-Phase and Solution-Phase Acidities. *J. Am. Chem. Soc.* **1993,** *115*, 12441–12445.

(7) Jungwirth, P.; Tobias, D. J. Ions at the Air/Water Interface. *J. Phys. Chem. B* **2002,** *106*, 6361–6373.

(8) Petersen, P. B.; Saykally, R. J. Adsorption of Ions to the Surface of Dilute Electrolyte Solutions: The Jones−Ray Effect Revisited. *J. Am. Chem. Soc.* **2005,** *127*, 15446–15452.

(9) Buch, V.; Milet, A.; Vacha, R.; Jungwirth, P.; Devlin, J. P. Water Surface Is Acidic. *Proc. Natl. Acad. Sci. U.S.A.* **2007,** *104*, 7342–7347.

(10) Hunter, E. P. L.; Lias, S. G. Evaluated Gas Phase Basicities and Proton Affinities of Molecules: An Update. *J. Phys. Chem. Ref. Data* **1998,** *27*, 413–656.

(11) Meot-Ner, M. The Ionic Hydrogen Bond. *Chem. Rev.* **2005,** *105*, 213–284.

(12) Aue, D. H.; Webb, H. M.; Bowers, M. T. Quantitative Proton Affinities, Ionization-Potentials, And Hydrogen Affinities of Alkylamines. *J. Am. Chem. Soc.* **1976,** *98*, 311–317.

(13) Aue, D. H.; Webb, H. M.; Bowers, M. T. Thermodynamic Analysis of Solvation Effects on Basicities of Alkylamines. An Electrostatic Analysis of Substituent Effects. *J. Am. Chem. Soc.* **1976,** *98*, 318–329.

(14) Popper, K. R. *The Logic of Scientific Discovery*; Hutchinson: London, 1972.

(15) Enami, S.; Hoffmann, M. R.; Colussi, A. J. Acidity Enhances the Formation of a Persistent Ozonide at Aqueous Ascorbate/Ozone Gas Interfaces. *Proc. Natl. Acad. Sci. U.S.A.* **2008,** *105*, 7365–7369.

(16) Enami, S.; Hoffmann, M. R.; Colussi, A. J. How Phenol and Alpha-Tocopherol React with Ambient Ozone at Gas/Liquid Interfaces. *J. Phys. Chem. A* **2009,** *113*, 7002–7010.

(17) Psillakis, E.; Cheng, J.; Hoffmann, M. R.; Colussi, A. J. Enrichment Factors of Perfluoroalkyl Oxoanions at the Air/Water Interface. *J. Phys. Chem. A* **2009,** *113*, 8826–8829.

(18) Cheng, J.; Hoffmann, M. R.; Colussi, A. J. Anion Fractionation and Reactivity at Air/Water:Methanol Interfaces. Implications for the Origin of Hofmeister Effects. *J. Phys. Chem. B* **2008,** *112*, 7157–7161.

(19) Enami, S.; Vecitis, C. D.; Cheng, J.; Hoffmann, M. R.; Colussi, A. J. Global Inorganic Source of Atmospheric Bromine. *J. Phys. Chem. A* **2007,** *111*, 8749–8752.

(20) Cheng, J.; Psillakis, E.; Hoffmann, M. R.; Colussi, A. J. Acid Dissociation versus Molecular Association of Perfluoroalkyl Oxoacids: Environmental Implications. *J. Phys. Chem. A* **2009,** *113*, 8152–8156.

(21) Shi, Q.; Davidovits, P.; Jayne, J. T.; Worsnop, D. R.; Kolb, C. E. Uptake of Gas-Phase Ammonia. 1. Uptake by Aqueous Surfaces As a Function of pH. *J. Phys. Chem. A* **1999,** *103*, 8812–8823.

(22) Swartz, E.; Shi, Q.; Davidovits, P.; Jayne, J. T.; Worsnop, D. R.; Kolb, C. E. Uptake of Gas-Phase Ammonia. 2. Uptake by Sulfuric Acid Surfaces. *J. Phys. Chem. A* **1999,** *103*, 8824–8833.

(23) Dole, M. A Theory of Surface Tension of Aqueous Solutions. *J. Am. Chem. Soc.* **1938,** *60*, 904–911.

(24) Manciu, M.; Ruckenstein, E. Specific Ion Effects via Ion Hydration: I. Surface Tension. *Adv. Colloid Interface Sci.* **2003,** *105*, 63–101.

(25) Israelachvilii, J. *Intermolecular & Surface Forces*, 2nd ed.; Academic Press: London, 1992.

(26) Gray-Weale, A.; Beattie, J. K. An Explanation for the Charge on Water's Surface. *Phys. Chem. Chem. Phys.* **2009,** *11*, 10994–11005.

(27) Creux, P.; Lachaise, J.; Graciaa, A.; Beattie, J. K. Specific Cation Effects at the Hydroxide-Charged Air/Water Interface. *J. Phys. Chem. C* **2007,** *111*, 3753–3755.

(28) Petersen, P. B.; Saykally, R. J. Evidence for an Enhanced Hydronium Concentration at the Liquid Water Surface. *J. Phys. Chem. B* **2005,** *109*, 7976–7980.

(29) Jarvis, N. L.; Scheiman, M. A. Surface Potentials of Aqueous Electrolyte Solutions. *J. Phys. Chem.* **1968,** *72*, 74–78.

(30) Manciu, M.; Ruckenstein, E. Ions at the Air/Water Interface. *J. Colloid Interface Sci.* **2006,** *304*, 541–544.

(31) Berry, R. S.; Rice, S. A.; Ross, J. *Physical Chemistry*; Wiley: New York, 1980.

(32) Boero, M.; Ikeshoji, T.; Terakura, K. Density and Temperature Dependence of Proton Diffusion in Water: A First-Principles Molecular Dynamics Study. *ChemPhysChem* **2005,** *6*, 1775–1779.

(33) Mmereki, B. T.; Hicks, J. M.; Donaldson, D. J. Adsorption of Atmospheric Gases at the Air−Water Interface. 3: Methylamines. *J. Phys. Chem. A* **2000,** *104*, 10789–10793.

(34) Harper, K.; Minofar, B.; Sierra-Hernandez, M. R.; Casillas-Ituarte, N. N.; Roeselova, M.; Allen, H. C. Surface Residence and Uptake of Methyl Chloride and Methyl Alcohol at the Air/Water Interface Studied by Vibrational Sum Frequency Spectroscopy and Molecular Dynamics. *J. Phys. Chem. A* **2009,** *113*, 2015–2024.

(35) Davidovits, P.; Kolb, C. E.; Williams, L. R.; Jayne, J. T.; Worsnop, D. R. Mass Accommodation and Chemical Reactions at Gas−Liquid Interfaces. *Chem. Rev.* **2006,** *106*, 1323–1354.

(36) Gilligan, J. J.; Lampe, F. W.; Nguyen, V. Q.; Vieira, N. E.; Yergey, A. L. Hydration of Alkylammonium Ions in the Gas Phase. *J. Phys. Chem. A* **2003,** *107*, 3687–3691.

(37) Rais, J.; Okada, T. Quantized Hydration Energies of Ions and Structure of Hydration Shell from the Experimental Gas-Phase Data. *J. Phys. Chem. B* **2008,** *112*, 5393–5402.

DOI: 10.1021/jz100322w | *J. Phys. Chem. Lett.* **2010,** *1*, 1599–1604

(38) Mmereki, B. T.; Donaldson, D. J. Ab Initio and Density Functional Study of Complexes between the Methylamines and Water. *J. Phys. Chem. A* **2002,** *106*, 3185–3190.
(39) Arshadi, M.; Kebarle, P. Hydration of OH^- and O_2^- in the Gas Phase. Comparative Solvation of OH^- By Water and the Hydrogen Halides. Effect of Acidity. *J. Phys. Chem.* **1970,** *74*, 1483–1485.
(40) Park, S. C.; Kim, J. K.; Lee, C. W.; Kang, H. Acid−Base Chemistry at the Ice Surface: Reverse Correlation between Intrinsic Basicity and Proton-Transfer Efficiency to Ammonia and Methyl Amines. *ChemPhysChem* **2007,** *8*, 2520–2525.
(41) Geissler, P. L.; Dellago, C.; Chandler, D.; Hutter, J.; Parrinello, M. Autoionization in Liquid Water. *Science* **2001,** *291*, 2121–2124.
(42) Beattie, J. K.; Djerdjev, A. N.; Warr, G. G. The Surface of Neat Water Is Basic. *Faraday Discuss.* **2009,** *141*, 31–39.
(43) Creux, P.; Lachaise, J.; Graciaa, A.; Beattie, J. K.; Djerdjev, A. M. Strong Specific Hydroxide Ion Binding at the Pristine Oil/Water and Air/Water Interfaces. *J. Phys. Chem. B* **2009,** *113*, 14146–14150.
(44) Cheng, J.; Vecitis, C.; Hoffmann, M. R.; Colussi, A. J. Experimental Anions Affinities for the Air/Water Interface. *J. Phys. Chem. B* **2006,** *110*, 25598–25602.
(45) McCarty, L. S.; Whitesides, G. M. Electrostatic Charging Due to Separation of Ions at Interfaces: Contact Electrification of Ionic Electrets. *Angew. Chem., Int. Ed.* **2008,** *47*, 2188–2207.
(46) Tian, C. S.; Ji, N.; Waychunas, G. A.; Shen, Y. R. Interfacial Structures of Acidic and Basic Aqueous Solutions. *J. Am. Chem. Soc.* **2008,** *130*, 13033–13039.
(47) Tian, C. S.; Shen, Y. R. Isotopic Dilution Study of the Water/Vapor Interface by Phase-Sensitive Sum-Frequency Vibrational Spectroscopy. *J. Am. Chem. Soc.* **2009,** *131*, 2790–2791.
(48) Ishiyama, T.; Morita, A. Analysis of Anisotropic Local Field in Sum Frequency Generation Spectroscopy with the Charge Response Kernel Water Model. *J. Chem. Phys.* **2009**, *131*, doi: 244714 10.1063/1.3279126.
(49) Tarbuck, T. L.; Ota, S. T.; Richmond, G. L. Spectroscopic Studies of Solvated Hydrogen and Hydroxide Ions at Aqueous Surfaces. *J. Am. Chem. Soc.* **2006,** *128*, 14519–14527.
(50) Levering, L. M.; Sierra-Hernandez, M. R.; Allen, H. C. Observation of Hydronium Ions at the Air−Aqueous Acid Interface: Vibrational Spectroscopic Studies of Aqueous HCI, HBr, and HI. *J. Phys. Chem. C* **2007,** *111*, 8814–8826.
(51) Petersen, P. B.; Saykally, R. J. Is the Liquid Water Surface Basic or Acidic? Macroscopic vs. Molecular-Scale Investigations. *Chem. Phys. Lett.* **2008,** *458*, 255–261.
(52) Tian, C. S.; Shen, Y. R. Sum-Frequency Vibrational Spectroscopic Studies of Water/Vapor Interfaces. *Chem. Phys. Lett.* **2009,** *470*, 1–6.
(53) Petersen, M. K.; Iyengar, S. S.; Day, T. J. F.; Voth, G. A. The Hydrated Proton at the Water Liquid/Vapor Interface. *J. Phys. Chem. B* **2004,** *108*, 14804–14806.
(54) Iuchi, S.; Chen, H. N.; Paesani, F.; Voth, G. A. Hydrated Excess Proton at Water−Hydrophobic Interfaces. *J. Phys. Chem. B* **2009,** *113*, 4017–4030.
(55) Mundy, C. J.; Kuo, I. F. W.; Tuckerman, M. E.; Lee, H. S.; Tobias, D. J. Hydroxide Anion at the Air−Water Interface. *Chem. Phys. Lett.* **2009,** *481*, 2–8.
(56) Mucha, M.; Frigato, T.; Levering, L. M.; Allen, H. C.; Tobias, D. J.; Dang, L. X.; Jungwirth, P. Unified Molecular Picture of the Surfaces of Aqueous Acid, Base, And Salt Solutions. *J. Phys. Chem. B* **2005,** *109*, 7617–7623.
(57) Winter, B.; Faubel, M.; Vacha, R.; Jungwirth, P. Behavior of Hydroxide at the Water/Vapor Interface. *Chem. Phys. Lett.* **2009,** *474*, 241–247.
(58) Zangi, R.; Engberts, J. Physisorption of Hydroxide Ions from Aqueous Solution to a Hydrophobic Surface. *J. Am. Chem. Soc.* **2005,** *127*, 2272–2276.
(59) Kudin, K. N.; Car, R. Why are Water−Hydrophobic Interfaces Charged?. *J. Am. Chem. Soc.* **2008,** *130*, 3915–3919.

DOI: 10.1021/jz100322w | *J. Phys. Chem. Lett.* **2010,** *1*, 1599–1604